

Generalized Separable Nonnegative Matrix Factorization

Junjun Pan Nicolas Gillis*

Department of Mathematics and Operational Research
Faculté Polytechnique, Université de Mons
Rue de Houdain 9, 7000 Mons, Belgium

Abstract

Nonnegative matrix factorization (NMF) is a linear dimensionality technique for nonnegative data with applications such as image analysis, text mining, audio source separation and hyperspectral unmixing. Given a data matrix M and a factorization rank r , NMF looks for a nonnegative matrix W with r columns and a nonnegative matrix H with r rows such that $M \approx WH$. NMF is NP-hard to solve in general. However, it can be computed efficiently under the separability assumption which requires that the basis vectors appear as data points, that is, that there exists an index set \mathcal{K} such that $W = M(:, \mathcal{K})$. In this paper, we generalize the separability assumption: We only require that for each rank-one factor $W(:, k)H(k, :)$ for $k = 1, 2, \dots, r$, either $W(:, k) = M(:, j)$ for some j or $H(k, :) = M(i, :)$ for some i . We refer to the corresponding problem as generalized separable NMF (GS-NMF). We discuss some properties of GS-NMF and propose a convex optimization model which we solve using a fast gradient method. We also propose a heuristic algorithm inspired by the successive projection algorithm. To verify the effectiveness of our methods, we compare them with several state-of-the-art separable NMF algorithms on synthetic, document and image data sets.

Keywords. nonnegative matrix factorization, separability, algorithms

1 Introduction

Given a nonnegative matrix $M \in \mathbb{R}_+^{m \times n}$ and an integer factorization rank r , nonnegative matrix factorization (NMF) is the problem of computing $W \in \mathbb{R}_+^{n \times r}$ and $H \in \mathbb{R}_+^{r \times m}$ such that $M \approx WH$. Typically, the columns of the input matrix M correspond to data points (such as images of pixel intensities or documents of word counts) and NMF allows to perform linear dimensionality reduction. In fact, we have $M(:, j) \approx \sum_{k=1}^r W(:, k)H(k, j)$ for all j , where $M(:, j)$ denotes the j th column of M . This means that the data points are approximated by points within an r -dimensional subspace spanned by the columns of W . The nonnegativity constraints lead to easily interpretable factors with applications such as image processing, text mining, hyperspectral unmixing and audio source separation; see for example the recent survey [11] and the references therein.

NMF is NP-hard in general [36] and its solution is in most cases not unique; see [11] and the references therein. These two issues motivated the introduction of the separability assumption as a way to solve NMF efficiently and have unique solutions. A matrix $M \in \mathbb{R}^{m \times n}$ is r -separable if there exist an index set \mathcal{K} of cardinality r and a nonnegative matrix H such that $M = M(:, \mathcal{K})H$, where $M(:, \mathcal{K})$ is the matrix containing the columns of M with index in \mathcal{K} . This means that there

*Emails: {junjun.pan, nicolas.gillis}@umons.ac.be. This work was supported by the European Research Council (ERC starting grant no 679515), and the Fonds de la Recherche Scientifique - FNRS and the Fonds Wetenschappelijk Onderzoek - Vlaanderen (FWO) under EOS Project no O005318F-RG47.

exists an NMF (W, H) such that each column of W is equal to a column of M . Given a matrix M that satisfies the separability condition, computing $W = M(:, \mathcal{K})$ and H can be done efficiently; see for example [14] and the references therein. The corresponding problem is referred to as separable NMF.

Let us present an equivalent definition of separability that will be particularly useful in this paper. It was originally proposed in [8, 9, 32] in order to design convex formulations for separable NMF. The matrix M is r -separable if there exist some permutation matrix $\Pi \in \{0, 1\}^{n \times n}$ and a nonnegative matrix $H' \in \mathbb{R}_+^{r \times (n-r)}$ such that

$$M\Pi = M\Pi \begin{pmatrix} I_r & H' \\ 0_{n-r, r} & 0_{n-r, n-r} \end{pmatrix},$$

where I_r is the r -by- r identity matrix and $0_{r,p}$ is the matrix of all zeros of dimension r by p . In fact, under an appropriate permutation, the first r columns of M correspond to the columns of W while the last $n-r$ columns are convex combinations of these first r columns. Equivalently, we have

$$M = M \underbrace{\Pi \begin{pmatrix} I_r & H' \\ 0_{n-r, r} & 0_{n-r, n-r} \end{pmatrix} \Pi^T}_{X \in \mathbb{R}^{n \times n}}. \quad (1)$$

Convex formulations were obtained by trying to find a matrix X such that (i) $M \approx MX$ and (ii) X has as many zero rows as possible [8, 9, 17, 32]; see Section 3 for more details.

Note that every m -by- n nonnegative matrix is n -separable since $M = MI_n$ hence it is important to find the minimal r . Geometrically, in noiseless conditions, the minimal r is the number of extreme rays of the cone generated by the columns of M .

Under the separability assumption, NMF can be solved in polynomial time. This has been known and used for a long time in the hyperspectral community; see [25] and the references therein. Furthermore, separable NMF can still be solved in polynomial time in the presence of noise [3, 4], and many robust algorithms have been proposed recently [2, 12, 13, 19, 32]. The separability assumption makes sense in several practical situations. In hyperspectral unmixing, each column of the data matrix is the spectral signature of a pixel. Separability requires that for each material present in the hyperspectral image, there exists a pixel that contains only that material; see for example [25]. In audio source separation, the input matrix is the time frequency amplitude spectrogram [10]. Separability requires that for each source, there exists a moment in time when only that source is active. In document classification, each entry $M(i, j)$ of matrix M indicates the importance of word i in document j (e.g., the number of occurrences of word i in document j). Separability of M (that is, each column of W appears as a column of M) requires that, for each topic, there exists at least one document only discuss that topic (a “pure” document). Separability of M^T (that is, each row of H appears as a row of M) requires that, for each topic, there exists at least one word used only in that topic [5] (a “pure” word, referred to as an anchor word).

In this paper, we generalize the separability assumption as follows.

Definition 1. A matrix $M \in \mathbb{R}_+^{m \times n}$ is (r_1, r_2) -separable if there exist an index set \mathcal{K}_1 of cardinality r_1 and an index set \mathcal{K}_2 of cardinality r_2 , and nonnegative matrices $P_1 \in \mathbb{R}_+^{r_1 \times n}$ and $P_2 \in \mathbb{R}_+^{m \times r_2}$ such that

$$M = M(:, \mathcal{K}_1)P_1 + P_2M(\mathcal{K}_2, :), \quad (2)$$

where $P_1(:, \mathcal{K}_1) = I_{r_1}$ and $P_2(\mathcal{K}_2, :) = I_{r_2}$.

We will refer to such matrices as generalized separable (GS) matrices, with their corresponding GS decomposition (2).

The (r_1, r_2) -separability is a natural extension of r -separability since a matrix is r -separable if and only if it is $(r, 0)$ -separable. Note that every m -by- n nonnegative matrix M is $(n, 0)$ - and $(0, m)$ -separable.

Generalized separability makes sense in several applications. In document classification, it requires that for each topic, there exists either

- a document discussing only that topic (a “pure” document), or
- a word used only by that topic (an anchor word).

In other terms, the r_1 columns of M indexed by \mathcal{K}_1 are r_1 pure documents, and the r_2 rows of M indexed by \mathcal{K}_2 are r_2 anchor words, for a total of $r = r_1 + r_2$ topics.

The conditions $P_1(:, \mathcal{K}_1) = I_{r_1}$ and $P_1(\mathcal{K}_2, :) = I_{r_2}$ are rather natural and mean that the pure documents and anchor words are represented by themselves. In terms of audio source separation [10], generalized separability requires that for each source there exists either

- a moment in time where only that source is active, or
- a frequency where only that source has a positive signature.

Related problems GS-NMF is related to the CUR decomposition and the pseudo-skeleton approximation. Given a matrix M , these techniques try to identify a subset of columns \mathcal{K}_1 and rows \mathcal{K}_2 of M such that $\|M - M(:, \mathcal{K}_1)UM(\mathcal{K}_2, :)\|_F$ is as small as possible. In the CUR decomposition, U is chosen so as to minimize the reconstruction error, that is, $U = M(:, \mathcal{K}_1)^\dagger MM(\mathcal{K}_2, :)^{\dagger}$, where A^\dagger denotes a Moore-Penrose generalized inverse of the matrix A [26]. In the skeleton approximation, $U = M(\mathcal{K}_2, \mathcal{K}_1)^{-1}$ [20]. We refer the reader to [27] and the references therein for more information on these models. Since these models do not take nonnegativity into account, their analysis is rather different than GS-NMF. For example, to obtain exact decompositions of a rank- r matrix, they can pick any subset of r linearly independent rows and columns; this is not true for GS-NMF.

GS-NMF is also related to a model introduced in [24] and referred to as latent low-rank representation (LatLRR). The goal is to represent the input matrix M as $M = MX + YM$ where both X and Y have low-rank. Intuitively, M is represented using a subspace of the column space of M (namely, MX) and a subspace of the row space (namely, YM). To achieve this goal, Liu and Yan [24] minimize the nuclear norms of X and Y (since minimizing the rank is hard in general) and apply their model on facial images. GS-NMF clearly shares some similarity with LatLRR. In fact, our convex model introduced in Section 3 will also use the representation $M = MX + YM$ but the constraints on X and Y will be rather different. Moreover, GS-NMF takes nonnegativity into account, and it is more interpretable as the basis used to reconstruct M cannot be any linear combinations of the columns/rows of M as in LatLRR, but need to be a subset of these columns/rows. For example, when applied on facial images (see Section 5.3 for numerical experiments), our model will identify important pixels and images within a data set (meaning that they can be used to approximate well all other images) while LatLRR identifies important linear combinations of pixels and images which is more difficult to interpret.

Outline and contribution of the paper In this paper, we consider the NMF problem under the generalized separability condition, referred to as generalized separable NMF (GS-NMF).

In Section 2, we provide an equivalent characterization of GS matrices, similarly as done for separable matrices in (1). This leads to an idealized model to tackle GS-NMF. We then present several properties of GS matrices. We present a class of m -by- n matrices which are not $(n - 1, 0)$ - nor $(0, m - 1)$ -separable but that are $(3, 3)$ -separable. This illustrates the fact that GS decompositions can be much more compact than separable ones, requiring much fewer rank-one

factors to reconstruct the input matrix. We also discuss non-uniqueness issues of GS-NMF, a problem which is not present for separable NMF. In Section 3, we propose a convex optimization model to tackle GS-NMF. It is the generalization of the models proposed in [17, 32] for separable NMF. Then, we implement a fast gradient method to tackle this model hence solve GS-NMF, similarly as done in [18] for separable NMF. Unfortunately, this model requires the use of $n^2 + m^2$ variables hence is computationally rather expensive and does not scale well for large data sets. In Section 4, we propose a heuristic algorithm inspired by the successive projection algorithm (SPA) [1, 19] which we refer to as the generalized successive projection algorithm (GSPA) and that requires $O(mnr)$ operations as for most NMF algorithms.

In Section 5, we perform extensive numerical experiments on synthetic, document and image data sets. In most cases, we will observe that GS-NMF algorithms are able to compute decompositions with the same number of rank-one factors but with a lower reconstruction error than separable NMF algorithms.

2 Properties of Generalized Separable Matrices

Let us first show a simple property.

Property 1 (Pattern of zeros). *Let $M \in \mathbb{R}_+^{m \times n}$ be (r_1, r_2) -separable as described in Definition 1 so that $M = M(:, \mathcal{K}_1)P_1 + P_2M(\mathcal{K}_2, :)$. Then $M(\mathcal{K}_2, \mathcal{K}_1) = 0_{r_2, r_1}$.*

Proof. According to (2), we have

$$M(\mathcal{K}_2, \mathcal{K}_1) = M(\mathcal{K}_2, \mathcal{K}_1)P_1(:, \mathcal{K}_1) + P_2(\mathcal{K}_2, :)M(\mathcal{K}_2, \mathcal{K}_1) = M(\mathcal{K}_2, \mathcal{K}_1) + M(\mathcal{K}_2, \mathcal{K}_1),$$

since, by definition, $P_1(:, \mathcal{K}_1) = I_{r_1}$ and $P_2(\mathcal{K}_2, :) = I_{r_2}$. This implies that $M(\mathcal{K}_2, \mathcal{K}_1) = 0$. \square

Intuitively, in terms of topic modeling for example, Property 1 means that a pure document about a topic cannot contain an anchor word from another topic.

Let us provide two equivalent characterization of GS matrices.

Property 2 (Equivalent characterization 1). *A matrix $M \in \mathbb{R}_+^{m \times n}$ is (r_1, r_2) -separable if and only if it can be written as*

$$M = \Pi_r \begin{pmatrix} W_1 & W_1H_1 + W_2H_2 \\ 0_{r_2, r_1} & H_2 \end{pmatrix} \Pi_c, \quad (3)$$

for some permutations matrices $\Pi_c \in \{0, 1\}^{n \times n}$ and $\Pi_r \in \{0, 1\}^{m \times m}$, and for some nonnegative matrices $W_1 \in \mathbb{R}_+^{m-r_2 \times r_1}$, $H_1 \in \mathbb{R}_+^{r_1 \times (n-r_1)}$, $W_2 \in \mathbb{R}_+^{(m-r_2) \times r_2}$ and $H_2 \in \mathbb{R}_+^{r_2 \times (n-r_1)}$.

Proof. This follows directly from Property 1 and Definition 1. The permutation Π_c is chosen such that it moves the columns of M corresponding to \mathcal{K}_1 in the first r_1 positions, and the permutation Π_r is chosen such that it moves the rows of M corresponding to \mathcal{K}_2 in the last r_2 positions. After these permutations, there is r_2 -by- r_1 block of zeros at the bottom left of $\Pi_r^T M \Pi_c^T$ since $M(\mathcal{K}_2, \mathcal{K}_1) = 0$ (Property 1). Moreover, since $M = M(:, \mathcal{K}_1)P_1 + P_2M(\mathcal{K}_2, :)$ for some nonnegative matrices P_1 and P_2 , we can take W_1, H_1, W_2 and H_2 such that $M(:, \mathcal{K}_1) = [W_1; 0_{r_2, r_1}]$, $P_1 = [I_{r_1} \ H_1]\Pi_c$, $M(\mathcal{K}_2, :) = [0_{r_2, r_1} \ H_2]$, and $P_2 = \Pi_r[W_2; I_{r_2}]$. \square

As explained in the introduction, a matrix M is r -separable if and only if it can be written as $M = MX$ where X has r non-zero rows. A similar characterization is possible for GS matrices.

Property 3 (Equivalent characterization 2). *A matrix $M \in \mathbb{R}_+^{m \times n}$ is (r_1, r_2) -separable if and only if it can be written as*

$$M = MX + YM,$$

where

$$X = \Pi_c^T \begin{pmatrix} I_{r_1} & H_1 \\ 0_{n-r_1, r_1} & 0_{n-r_1, n-r_1} \end{pmatrix} \Pi_c, \quad Y = \Pi_r \begin{pmatrix} 0_{m-r_2, m-r_2} & W_2 \\ 0_{r_2, m-r_2} & I_{r_2} \end{pmatrix} \Pi_r^T, \quad (4)$$

for some permutations matrices $\Pi_c \in \{0, 1\}^{n \times n}$ and $\Pi_r \in \{0, 1\}^{m \times m}$, and for some $H_1 \in \mathbb{R}_+^{r_1 \times (n-r_1)}$ and $W_2 \in \mathbb{R}_+^{(m-r_2) \times r_2}$.

Proof. By Property 2, the matrix M is (r_1, r_2) -separable if and only if there exist some permutation matrices $\Pi_c \in \{0, 1\}^{n \times n}$ and $\Pi_r \in \{0, 1\}^{m \times m}$ such that

$$M = \Pi_r \begin{pmatrix} W_1 & W_1 H_1 + W_2 H_2 \\ 0_{r_2, r_1} & H_2 \end{pmatrix} \Pi_c, \quad (5)$$

for some $W_1 \in \mathbb{R}_+^{(m-r_2) \times r_1}$, $H_1 \in \mathbb{R}_+^{r_1 \times (n-r_1)}$, $W_2 \in \mathbb{R}_+^{(m-r_2) \times r_2}$, $H_2 \in \mathbb{R}_+^{r_2 \times (n-r_1)}$. Letting $\tilde{M} = \Pi_r^T M \Pi_c^T$ hence $M = \Pi_r \tilde{M} \Pi_c$, we have

$$\tilde{M} = \tilde{M} \begin{pmatrix} I_{r_1} & H_1 \\ 0_{n-r_1, r_1} & 0_{n-r_1, n-r_1} \end{pmatrix} + \begin{pmatrix} 0_{m-r_2, m-r_2} & W_2 \\ 0_{r_2, m-r_2} & I_{r_2} \end{pmatrix} \tilde{M}.$$

□

In practice, given a GS matrix, it is important to decompose it as a (r_1, r_2) -separable matrix with minimal value for $r_1 + r_2$ since this compresses the data the most. In the following, minimal (r_1, r_2) -separable matrices are defined.

Definition 2. A matrix M is a minimal (r_1, r_2) -separable if M is (r_1, r_2) -separable and M is not (r'_1, r'_2) -separable for any $r'_1 + r'_2 < r_1 + r_2$.

By property 3, finding minimal GS decompositions is equivalent to finding X and Y that satisfy (4) and such that the number of non-zero rows of X and non-zero columns of Y is minimized.

Property 4 (Idealized model). *Let M be minimal (r_1, r_2) -separable, and let (X^*, Y^*) be an optimal solution of*

$$\min_{X \in \mathbb{R}_+^{n \times n}, Y \in \mathbb{R}_+^{m \times m}} \|X\|_{row,0} + \|Y\|_{col,0} \quad \text{such that } M = MX + YM, \quad (6)$$

where $\|X\|_{row,0}$ equal to the number of nonzero rows of X and $\|Y\|_{col,0}$ equals to the number of nonzero columns of Y . Let also \mathcal{K}_1 correspond to the indices of the non-zero rows of X^* and \mathcal{K}_2 to the indices of the non-zero columns of Y^* . If $\text{rank}(M) = r_1 + r_2$, we have

$$\|X^*\|_{row,0} + \|Y^*\|_{col,0} = |\mathcal{K}_1| + |\mathcal{K}_2| = r_1 + r_2.$$

Proof. By Property 3, an (r_1, r_2) -separable matrix can be written as $M = MX + YM$ where the number of non-zero rows of X and non-zero columns of Y is $r_1 + r_2$. Hence, by optimality of (X^*, Y^*) , we have $|\mathcal{K}_1| + |\mathcal{K}_2| \leq r_1 + r_2$.

Moreover, since $\text{rank}(M) = r_1 + r_2$, we must have $|\mathcal{K}_1| + |\mathcal{K}_2| \geq r_1 + r_2$. □

Some remarks are in order:

- As opposed to separable NMF, due to the non-uniqueness of GS-NMF, $|\mathcal{K}_1|$ is not necessarily equal to r_1 and $|\mathcal{K}_2|$ to r_2 ; see Property 9 below.
- Unfortunately, solving (6) does not guarantee X and Y to have the form (4) where X and Y contain the identity matrix as a submatrix. This is why we need the condition $\text{rank}(M) = r_1 + r_2$.
- Of course, (6) is a difficult combinatorial problem. We will consider in Section 3 a convex relaxation. Before doing that, we first present several other interesting properties of GS matrices.

From a practical point of view, GS matrices will be particularly interesting when they allow to compress the data significantly more than separable matrices. In other words, it would be interesting to know whether there exists (r_1, r_2) -separable matrices which are not $(r, 0)$ - nor $(0, r)$ -separable for $r \gg r_1 + r_2$. In fact, this is the case; see Property 5 for the case $r_1 = r_2 = 3$ and $r = \min(m - 1, n - 1)$. First let show the following lemma.

Lemma 1. *There exist 3-by- n matrices that are $(2, 1)$ -separable but not $(n - 1, 0)$ -separable.*

Proof. Consider the 3-by- n matrix

$$M_n = \begin{pmatrix} 1 & 0 & \frac{1}{2} & 0 & x^T \\ 0 & 1 & 0 & \frac{1}{2} & y^T \\ 0 & 0 & \frac{1}{2} & \frac{1}{2} & z^T \end{pmatrix} \quad (7)$$

where $x, y, z \in \mathbb{R}^{n-4}$ are such that (x_i, y_i, z_i) for $i = 1, 2, \dots, n - 4$ are defined as $0 < x_i < \frac{1}{2}$ and $x_i \neq x_j$ for all $i \neq j$, $y_i = 2(\frac{1}{2} - x_i)^2$, $z_i = 1 - x_i - y_i$. The points (x_i, y_i, z_i) are distinct points on a curve on the unit simplex hence such points cannot be written as conic combinations of any other points on that curve. In fact, since the entries of the vectors (x_i, y_i, z_i) 's sum to one, the weights in such a conic combination would also have to sum to one hence such a conic combination would actually be a convex combination. Clearly, distinct points on the circle (x_i, y_i) 's are not convex combination of one another; in other words, every such point is a vertex of their convex hull.

Note also that the third and fourth column of M_n are the two extreme points of that curve. The first column of M_n also cannot be written as a convex combination of all the other columns since $z_i \neq 0$ for all i . This implies that M_n is not $(n - 1, 0)$ separable: every column of M_n is an extreme ray of the cone spanned by the columns of M_n . Moreover, M_n is $(2, 1)$ -separable since $M_n(1 : 2, 1 : 2) = I_r$ while the third row can be approximated by itself: we have

$$M_n = M_n(:, 1 : 2)P_1 + P_2M_n(3, :),$$

where $P_1 = M_n(1 : 2, :)$, $P_2 = (0, 0, 1)^T$. □

Property 5 (Compression). *There exist m -by- n matrices that are $(3, 3)$ -separable but not $(n - 1, 0)$ - nor $(0, m - 1)$ -separable.*

Proof. Let M_n be a 3-by- n matrix and M_m be a 3-by- m matrix constructed as in (7). Let us also construct the $(m + 3)$ -by- $(n + 3)$ matrix

$$M = \begin{pmatrix} 0_{3,3} & M_n \\ M_m^T & 0_{m,n} \end{pmatrix}. \quad (8)$$

By Lemma 1, M is $(3, 3)$ -separable (note that the corresponding GS decomposition is not unique since M_n is $(2, 1)$ - and $(0, 3)$ -separable), while not being $(n + 2, 0)$ -separable nor $(0, m + 2)$ -separable.

In fact, assume M is $(0, m+2)$ -separable. Observe that any row that would be selected from the first 3 rows (resp. last m rows) of M cannot be used to reconstruct any of the last m rows (resp. first 3 rows) of M using a positive weight because of the zeros in the last positions (resp. in the first positions). Hence a $(0, m+2)$ -separable decomposition of M would imply that either M_m^T is $(0, m-1)$ -separable, a contradiction with Lemma 1, or that M_n is $(0, 2)$ -separable which is not possible since $\text{rank}(M_n) = 3$. The same observation holds for the columns, by symmetry of the problem. \square

The next property is rather straightforward but we state here for completeness. It shows that generalized separability is invariant to scaling.

Property 6 (Scaling). *The matrix M is (r_1, r_2) -separable if and only if $D_1 M D_2$ is (r_1, r_2) -separable for any diagonal matrices D_1 and D_2 whose diagonal elements are positive.*

Proof. Let M be (r_1, r_2) -separable. We have $M = M(:, \mathcal{K}_1)P_1 + P_2 M(\mathcal{K}_2, :)$ with $|\mathcal{K}_1| = r_1$ and $|\mathcal{K}_2| = r_2$. Multiplying on both sides by D_1 and D_2 , we obtain

$$D_1 M D_2 = D_1 M(:, \mathcal{K}_1)P_1 D_2 + D_1 P_2 M(\mathcal{K}_2, :)D_2.$$

Denoting $\tilde{M} = D_1 M D_2$, $\tilde{P}_1 = D_2(\mathcal{K}_1, \mathcal{K}_1)^{-1}P_1 D_2$ and $\tilde{P}_2 = D_1 P_2 D_1(\mathcal{K}_2, \mathcal{K}_2)^{-1}$, we have

$$\tilde{M} = \tilde{M}(:, \mathcal{K}_1)\tilde{P}_1 + \tilde{P}_2 \tilde{M}(\mathcal{K}_2, :),$$

where $\tilde{P}_1(\mathcal{K}_1, \mathcal{K}_1) = I_{r_1}$ and $\tilde{P}_2(\mathcal{K}_2, \mathcal{K}_2) = I_{r_2}$; hence \tilde{M} is (r_1, r_2) -separable. The proof in the other direction is the same since $\tilde{M} = D_1 M D_2$ is the diagonal scaling of M using the inverses of D_1 and D_2 . \square

Unicity of GS decompositions As opposed to separable NMF, GS-NMF does not necessarily admit a unique solution (up to scaling and permutation of the rank-one factors). In other words, for a minimal (r_1, r_2) -separable matrix M , the way of picking the rows and columns of M is not necessarily unique: it may also be (r_3, r_4) -separable with $r_3 + r_4 = r_1 + r_2$ where $r_1 \neq r_3$ and $r_2 \neq r_4$, or it can be (r_1, r_2) -separable with different selection of rows and columns; this is the case for example for the matrix M in (8).

The simplest cases are for rank-one and rank-two matrices.

Property 7 (Rank-one matrices). *Any nonnegative rank-one matrix is $(1, 0)$ - and $(0, 1)$ -separable.*

Proof. This follows directly from the fact that all rows (resp. columns) of a rank-one matrix are multiple of one another. \square

Property 8 (Rank-two matrices). *Any nonnegative rank-two matrix is $(2, 0)$ - and $(0, 2)$ -separable.*

Proof. This follows from the fact that any nonnegative rank-two matrix is 2-separable [34]. The reason is that a two-dimensional cone is always spanned by its two extreme rays. \square

Examples can be constructed for any values of (r_1, r_2) .

Property 9 (Construction of non-unique minimal (r_1, r_2) -separable matrices). *For any (r_1, r_2) , we can construct minimal (r_1, r_2) -separable matrices such that they are also minimal (r_3, r_4) -separable with $r_1 + r_2 = r_3 + r_4$, $r_3 \neq r_1$ and $r_4 \neq r_2$.*

Proof. Let $r_1 > r_3$, $r_2 < r_4$ and $r_1 + r_2 = r_3 + r_4$. Let also $M_{11} \in \mathbb{R}_+^{(m-r_4) \times r_3}$, $M_{22} \in \mathbb{R}_+^{(r_4-r_2) \times (r_1-r_3)}$ and $M_{33} \in \mathbb{R}_+^{r_2 \times (n-r_1)}$ be any nonnegative matrices. Let us construct M as follows:

$$M = \begin{pmatrix} M_{11} & 0_{m-r_4, r_1-r_3} & M_{13} \\ 0_{r_4-r_2, r_3} & M_{22} & M_{23} \\ 0_{r_2, r_3} & 0_{r_2, r_1-r_3} & M_{33} \end{pmatrix},$$

where

$$M_{13} = M_{11}X_1 + Y_1M_{33} \in \mathbb{R}_+^{(m-r_4) \times (n-r_1)} \quad \text{and} \quad M_{23} = M_{22}X_2 + Y_2M_{33} \in \mathbb{R}_+^{(r_4-r_2) \times (n-r_1)},$$

for any $X_1 \in \mathbb{R}_+^{r_3 \times (n-r_1)}$, $Y_1 \in \mathbb{R}_+^{(m-r_4) \times r_2}$, $X_2 \in \mathbb{R}_+^{(r_1-r_3) \times (n-r_1)}$, $Y_2 \in \mathbb{R}_+^{(r_4-r_2) \times r_2}$.

We have that M is (r_1, r_2) -separable where \mathcal{K}_1 contains the first r_1 columns of M and \mathcal{K}_2 contains the last r_2 rows of M since

$$\begin{pmatrix} M_{13} \\ M_{23} \end{pmatrix} = \begin{pmatrix} M_{11} & 0_{m-r_4, r_1-r_3} \\ 0_{r_4-r_2, r_3} & M_{22} \end{pmatrix} \begin{pmatrix} X_1 \\ X_2 \end{pmatrix} + \begin{pmatrix} Y_1 \\ Y_2 \end{pmatrix} M_{33},$$

Similarly, we have that M is (r_3, r_4) -separable where \mathcal{K}_1 contains the first r_3 columns of M and \mathcal{K}_2 contains the last r_4 rows of M since

$$\begin{pmatrix} 0_{m-r_4, r_1-r_3} & M_{13} \end{pmatrix} = M_{11} \begin{pmatrix} 0 & X_1 \end{pmatrix} + \begin{pmatrix} 0 & Y_1 \end{pmatrix} \begin{pmatrix} M_{22} & M_{23} \\ 0_{r_2, r_1-r_3} & M_{33} \end{pmatrix}.$$

□

The simplest example is for a 3-by-3 matrix that is $(2, 1)$ - and $(1, 2)$ -separable, and also trivially $(3, 0)$ - and $(0, 3)$ -separable:

$$\begin{pmatrix} 1 & 0 & 2 \\ 0 & 1 & 2 \\ 0 & 0 & 1 \end{pmatrix}.$$

We simply took $M_{11} = M_{22} = M_{33} = X_1 = X_2 = Y_1 = Y_2 = 1$ in Property 9.

In order to guarantee uniqueness, a possible way is to have a single pattern of zeros which is large enough.

Property 10 (Condition for uniqueness). *Let M be minimal (r_1, r_2) -separable and let M not be $(r_1 + r_2, 0)$ -separable nor $(0, r_1 + r_2)$ -separable. If M does not contain a pattern of zeros of size $r_3 r_4$ with $r_1 + r_2 = r_3 + r_4$, except for $M(\mathcal{K}_2, \mathcal{K}_1) = 0$, then M admits a unique GS decomposition of size (r_1, r_2) .*

Proof. This follows directly from Property 1. □

Further direction of research would be to understand GS matrices better and derive some other conditions that lead to unique decompositions.

3 Convex Optimization Model and Fast Gradient Method

In real data sets, due to the presence of noise (and model misfit), the model (6) should be modified to

$$\min_{X \in \mathbb{R}_+^{n \times n}, Y \in \mathbb{R}_+^{m \times m}} \|X\|_{\text{row}, 0} + \|Y\|_{\text{col}, 0} \quad \text{such that} \quad \|M - MX - YM\| \leq \epsilon, \quad (9)$$

where ϵ denotes the noise level. The norm of the residual $\|M - MX - YM\|$ can be chosen according to the noise statistic. In this paper, we will consider the Frobenius norm, that is, $\|M - MX - YM\|_F = \sum_{i,j} (M - MX - YM)_{i,j}^2$; see for example [7] for a discussion on the choice of the objective function.

3.1 Convex optimization model

As it is challenging to solve (9), it can be relaxed to a convex optimization model as follows:

$$\min_{X \in \mathbb{R}_+^{n \times n}, Y \in \mathbb{R}_+^{m \times m}} \|X\|_{1,q} + \|Y^T\|_{1,q} \quad \text{such that} \quad \|M - MX - YM\| \leq \epsilon, \quad (10)$$

where $\|X\|_{1,q} := \sum_{i=1}^n \|X(i, :)\|_q$ and $\|Y^T\|_{1,q} := \sum_{i=1}^n \|Y(:, i)\|_q$. The quantities $\|X\|_{1,q}$ and $\|Y^T\|_{1,q}$ are the ℓ_1 norm of the vector containing the l_q norms of the rows of X and the columns of Y , respectively. The model aims to generate a matrix X with only a few non-zero rows and a matrix Y with only a few non-zero columns. This model is a generalization of separable NMF convex relaxations: $q = 2$ was proposed in [8], while $q = +\infty$ was proposed in [9]. In fact, (10) coincides with the models from [8, 9] by taking $Y = 0$.

The rationale behind this model is that the ℓ_1 norm is the largest convex function smaller than ℓ_0 norm on the ℓ_∞ ball; see for example [31]. In other terms, $\|X\|_{1,q} \leq \|X\|_{row,0}$ as long as $\|X(i, :)\|_q \leq 1$ for all i .

Considering $q = +\infty$, $\|X(i, :)\|_q \leq 1$ holds for example for $X \leq 1$. This can be assumed without loss of generality given that the input matrix is properly scaled.

Definition 3. The matrix M is scaled if $\|M(:, j)\|_1 = k_1$ for all j and $\|M(i, :)\|_1 = k_2$ for all i , for some $nk_1 = mk_2 > 0$.

Given a nonnegative matrix M , it is in most cases possible to scale it, that is, find diagonal matrices D_r and D_c such that $M_s = D_r M D_c$ is scaled. It requires that the matrix M has sufficiently many non-zero elements. When the matrix is scalable, the algorithm that alternatively scales the columns and rows of M will converge to a scaled matrix. We refer the reader to [21, 30] for more details on this topic.

We have the following property.

Property 11. Let M be a scaled (r_1, r_2) -separable matrix. Then M can be decomposed as in (4) with

$$X(i, j) \leq X(i, i) \leq 1 \text{ for } 1 \leq i, j \leq n, \quad \text{and} \quad Y(l, t) \leq Y(t, t) \leq 1 \text{ for } 1 \leq l, t \leq m.$$

Proof. Using Property 2 we have, after proper permutations of the columns and rows of M , that

$$M = \begin{pmatrix} W_1 & W_1 H_1 + W_2 H_2 \\ 0_{r_2, r_1} & H_2 \end{pmatrix}.$$

Since M is scaled, we have $e^T M(:, j) = e^T W_1(:, j) = k_1$ for $1 \leq j \leq r_1$, where e is the vector of all one of appropriate dimension. For $j = r_1 + 1, \dots, n$, we have

$$k_1 = e^T M(:, j) \geq e^T W_1 H_1(:, j - r_1) = k_1 e^T H_1(:, j - r_1),$$

since all matrices involved are nonnegative. This implies that $H_1 \leq 1$. In fact, this implies the stronger condition $\|H_1(:, j)\|_1 \leq 1$ for all j . By symmetry, the same result holds for W_2 , that is,

$W_2 \leq 1$ and $\|W_2(i, :)\|_1 \leq 1$ for all i . Therefore, up to permutations, using the same derivations as in Property 3, we have

$$M = M \begin{pmatrix} I & H_1 \\ 0 & 0 \end{pmatrix} + \begin{pmatrix} 0 & I \\ 0 & W_2 \end{pmatrix} M,$$

where $H_1 \leq 1$ and $W_2 \leq 1$. \square

In this paper, we focus on another convex model to tackle GS-NMF. For a scaled GS matrix, it can be written as follows:

$$\begin{aligned} \min_{X \in \mathbb{R}_+^{n \times n}, Y \in \mathbb{R}_+^{m \times m}} \quad & \text{trace}(X) + \text{trace}(Y), \\ \text{such that} \quad & \|M - MX - YM\| \leq \epsilon, \\ & X(i, j) \leq X(i, i) \leq 1 \text{ for } 1 \leq i, j \leq n, \\ & Y(l, t) \leq Y(t, t) \leq 1 \text{ for } 1 \leq l, t \leq m. \end{aligned} \tag{11}$$

This model is the generalization of the model from [12] for separable matrices, which is an improvement of the model from [32]. The rationale behind this model is the following. Since X is nonnegative, minimizing its trace is equivalent to minimize the ℓ_1 norm of its diagonal entries, that is, $\text{trace}(X) = \|\text{diag}(X)\|_1$. Hence (11) promotes solutions whose diagonal is sparse. Then, the constraints $X(i, j) \leq X(i, i)$ for all i, j impose that the largest entry in each row is the corresponding diagonal entry. Hence, if a diagonal entry is equal to zero, the entire row is zero. This makes this model generate solutions that tend to be row sparse. Note that for any feasible solution X of (11), we have $\text{trace}(X) \leq \|X\|_{\text{row}, 0}$. In fact, since $0 \leq X(i, j) \leq X(i, i)$ for all i, j , $\|X\|_{1, \infty} = \text{trace}(X)$ for any X . Moreover, since $X \leq 1$, $\|X\|_{1, \infty} \leq \|X\|_{\text{row}, 0}$. By symmetry, we also have $\text{trace}(Y) \leq \|Y\|_{\text{col}, 0}$.

The model (11) can easily be generalized for non-scaled M ; see Section 3.2. Compared to (10), it has an important advantage: It is a smooth optimization problem, and the projection onto the feasible set can be performed efficiently, in $\mathcal{O}(n^2 \log n + m^2 \log m)$ operations [18]. Therefore, we can easily design first-order optimization method with strong convergence guarantees; see Section 3.2.

3.2 Fast Gradient Method for GS-NMF

Let us generalize the model (11) to non-scaled matrices, as done for separable matrices in [17]. Using essentially a similar argument as in the proof of Property 11, we have for a GS matrix M that for all j

$$M(:, j) \leq M(:, \mathcal{K}_1)P_1(:, j) \leq M(:, \mathcal{K}_1(k))P_1(k, j) \text{ for all } k,$$

since $M = M(:, \mathcal{K}_1)P_1 + P_2M(\mathcal{K}_2, :)$. Taking the ℓ_1 norm on both sides, we have

$$P_1(k, j) \leq \frac{\|M(:, j)\|_1}{\|M(:, \mathcal{K}_1(k))\|_1} \text{ for all } k, j.$$

A similar observation can be made for P_2 , which leads to the generalization of (11) for non-scaled matrices:

$$\min_{X \in \Omega_1, Y \in \Omega_2} \text{trace}(X) + \text{trace}(Y) \quad \text{such that} \quad \|M - MX - YM\| \leq \epsilon, \tag{12}$$

where the sets Ω_1 and Ω_2 are defined as

$$\Omega_1 = \{X \in \mathbb{R}_+^{n \times n} \mid X(i, i) \leq 1, w_i X(i, j) \leq w_j X(i, i) \text{ for all } i, j\},$$

$$\Omega_2 = \{Y \in \mathbb{R}_+^{m \times m} | Y(t, t) \leq 1, \hat{w}_t Y(l, t) \leq \hat{w}_l Y(t, t) \text{ for all } l, t\},$$

where the vector $w \in \mathbb{R}_+^n$ contains the l_1 norm of the columns M , that is, $w_j = \|M(:, j)\|_1$ for all $j = 1, \dots, n$, and the vector $\hat{w} \in \mathbb{R}_+^m$ contains the l_1 norm of the rows of M , that is, $\hat{w}_l = \|M(l, :)\|_1$ for all $l = 1, \dots, m$.

To solve the smooth convex problem (12), interior-point methods can be used for example using SDPT3 [35]. However using such second-order method to solve (12) which has $n^2 + m^2$ variables and as many constraints would be numerically expensive. Moreover, in our case, high accuracy solutions are not crucial: the main goal of solving (12) is to identify the important columns and rows of M which correspond to the largest entries in the diagonal entries of X and Y . Therefore, we use Nesterov's optimal first-order method [28, 29], namely, a fast gradient method, similarly as done in [18] for separable matrices. Here "fast" refers to the fact that it attains the best possible convergence rate of $\mathcal{O}(1/k^2)$ in the first-order regime. To do so, we consider the penalized version of (12):

$$\min_{X \in \Omega_1, Y \in \Omega_2} F(X, Y), \text{ with } F(X, Y) = \frac{1}{2} \|M - MX - YM\|_F^2 + \lambda (\text{trace}(X) + \text{trace}(Y)), \quad (13)$$

where $\lambda > 0$ is a penalty parameter which balances the importance between the approximation error $\|M - MX - YM\|_F^2$ and the sum of the traces of X and Y .

To initialize X and Y and set the value of λ , we adopt the following strategy described in Algorithm 1, similarly as in [18]:

- Extract a subset \mathcal{K}_1 of columns and a subset \mathcal{K}_2 of rows of M such that $|\mathcal{K}_1| + \mathcal{K}_2 = r$ using the heuristic algorithm referred to as GSPA; see Section 4.
- Compute the corresponding optimal weights (P_1^*, P_2^*) :

$$(P_1^*, P_2^*) = \underset{P_1 \in \mathbb{R}_+^{r_1 \times n}, P_2 \in \mathbb{R}_+^{m \times r_2}}{\text{argmin}} \|M - M(:, \mathcal{K}_1)P_1 - P_2 M(\mathcal{K}_2, :)\|_F^2.$$

We used the coordinate descent implemented in [15].

- Define $X_0(\mathcal{K}_1, :) = P_1^*$ and $Y_0(:, \mathcal{K}_2) = P_2^*$, while $X_0(i, :) = 0$ for $i \notin \mathcal{K}_1$ and $Y_0(:, j) = 0$ for $j \notin \mathcal{K}_2$.
- Set $\lambda = \tilde{\lambda} \frac{\|M - MX_0 - Y_0 M\|}{2r}$, where $r = r_1 + r_2$ and some $\tilde{\lambda}$. Typically, $\tilde{\lambda} \in [10^{-3}, 10]$ works well.

Algorithm 1 Initialization for GS-FGM

Input: $M \in \mathbb{R}_+^{m \times n}$, r , $\tilde{\lambda} > 0$.

Output: Initial solution $(X_0, Y_0) \in \mathbb{R}^{n \times n} \times \mathbb{R}^{m \times m}$ for (13), and parameter λ balancing the two terms in the objective.

- 1: $(\mathcal{K}_1, \mathcal{K}_1) = \text{GSPA}(M, r)$; see Algorithm 3;
 - 2: $(P_1^*, P_2^*) = \underset{P_1 \in \mathbb{R}_+^{r_1 \times n}, P_2 \in \mathbb{R}_+^{m \times r_2}}{\text{argmin}} \|M - M(:, \mathcal{K}_1)P_1 - P_2 M(\mathcal{K}_2, :)\|_F^2$;
 - 3: $X_0(\mathcal{K}_1, :) = 0_{n,n}$; $Y_0(:, \mathcal{K}_2) = 0_{m,m}$;
 - 4: $X_0(\mathcal{K}_1, :) = P_1^*$; $Y_0(:, \mathcal{K}_2) = P_2^*$;
 - 5: $\lambda = \tilde{\lambda} \frac{\|M - MX_0 - Y_0 M\|}{2r}$.
-

To solve model (13), we employ Algorithm 2 which is an optimal first-order method to minimize $F(X, Y)$ over the sets Ω_1 and Ω_2 . To compute the Euclidean projection of X on the set Ω_1 and

of Y on the set Ω_2 , we use the method proposed in [18], which only requires $\mathcal{O}(n^2 \log n)$ and $\mathcal{O}(m^2 \log m)$ operations for the projection of X and Y , respectively.

The main computational cost of Algorithm 2 resides in lines 2, 7 and 9. For line 2, the maximum singular value of M can be well approximated by the power method which needs $\mathcal{O}(mn)$ operations. In line 5, the computation of the different matrix products require $\mathcal{O}(mn^2 + m^2n)$ operations. For line 7, the projections of X and Y require $\mathcal{O}(n^2 \log n + m^2 \log m)$ [18]. Finally, Algorithm 2 requires $\mathcal{O}(mn^2 + m^2n)$ operations, assuming $m \geq \log n$ and $n \geq \log m$.

Algorithm 2 GS-NMF with a Fast Gradient Method (GS-FGM)

Input: A $M \in \mathbb{R}_+^{m \times n}$, number r_1 of columns and r_2 of rows to extract, and maximum number of iterations *maxiter*.

Output: Matrices X and Y solving (13), and a set $\mathcal{K}_1 \subset \{1, 2, \dots, n\}$ of column indices and a set $\mathcal{K}_2 \subset \{1, 2, \dots, m\}$ of row indices such that $\min_{P_1, P_2 \geq 0} \|M - M(:, \mathcal{K}_1)P_1 + P_2M(\mathcal{K}_2, :)\|_F$ is small.

```

1: % Initialization
2:  $\alpha_0 \leftarrow 0.05$ ;  $L \leftarrow 2\sigma_{\max}(M)^2$ ;
   Initialize  $X$ ,  $Y$  and  $\lambda$ ; see Algorithm 1.
3: for  $k = 1 : \text{maxiter}$  do
4:   % Keep previous iterates in memory
5:    $X_p \leftarrow X$ ;  $Y_p \leftarrow Y$ ;
6:   % Gradient computation
7:    $\nabla_X F(X, Y) \leftarrow M^T M X + M^T Y M - M^T M + \lambda I_n$ ;
    $\nabla_Y F(X, Y) \leftarrow M X M^T + Y M M^T - M M^T + \lambda I_m$ ;
8:   % Gradient step and projection
9:    $X \leftarrow P_\Omega(X - \frac{1}{L} \nabla_X F(X, Y))$ ;
    $Y \leftarrow P_\Omega(Y - \frac{1}{L} \nabla_Y F(X, Y))$ ;
10:  % Acceleration / Momentum step
11:   $X \leftarrow X + \beta_k(X - X_p)$ ;
    $Y \leftarrow Y + \beta_k(Y - Y_p)$ ;
   where  $\beta_k = \frac{\alpha_{k-1}(1-\alpha_{k-1})}{\alpha_{k-1}^2 + \alpha_k}$  such that  $\alpha_k \geq 0$  and  $\alpha_k^2 = (1 - \alpha_k)\alpha_{k-1}^2$ 
12: end for
13:  $\mathcal{K}_1 \leftarrow \text{post-process}(X, r_1)$ ;
    $\mathcal{K}_2 \leftarrow \text{post-process}(Y, r_2)$ .

```

We will refer to Algorithm 2 as GS-FGM. Note that the numbers r_1 and r_2 are given as input of Algorithm 2. However, they can also be detected automatically by identifying the entries on the diagonals of X and Y above a certain threshold. For simplicity, we will use the same two post-processing procedures as in [18]:

- For synthetic data sets, we simply pick the r_1 largest entries of the diagonals of X and the r_1 largest entries of the diagonals of Y .
- For real data sets, it is also important to consider off-diagonal entries of X and Y . The reason is that the input matrix can be far from being a GS matrix. For example, an outlying column will in general lead to a large diagonal entry in X (since an outlier is in general not well approximated with other data points) while the other entries on the same row will be close to zero (since an outlier is in general useless to reconstruct other data points). This means that if a row of X has many large entries, it is likely to be more important than a row with only a large diagonal entry. For this reason, we sort the columns of M by applying SPA

on X^T as done in [18]; an similarly for Y to sort the rows of M . It remains to decide how many column and row indices to pick in each of these ordered sets. To do so, we sequentially select a column or a row of M as follows: at each step, we will select the column/row of M such that the residual after projection onto its orthogonal complement is the smallest, and at the next step, we replace M by the corresponding residual; this shares some similarity with the algorithm presented in the next section.

4 Heuristic Algorithm for GS-NMF

Algorithm 2 is computationally expensive, and does not scale linearly with the dimension of the input matrix. For large-scale problems, it would not be applicable. When running on a standard computer, m and n should be limited to values below a thousand. A possible way to overcome this issue is to preselect, a priori, a subset of columns and rows of M , reducing the number of variables; see Section 5.2 for a discussion.

In this section, we derive a fast heuristic algorithm for GS-NMF. It is inspired from one of the most widely used separable NMF algorithm, namely the successive projection algorithm (SPA). SPA is essentially equivalent to QR with column pivoting; it was introduced in [1] in the context of spectral unmixing but has been rediscovered many times; see the discussions in [14, 25]. Moreover, SPA is robust in the presence of noise [19]. SPA assumes that the input matrix has the form $M = M(:, \mathcal{K})[I_r, H']\Pi$ where Π is a permutation matrix and $H' \geq 0$ and $\|H'(:, j)\|_1 \leq 1$ for all j . This means that the columns of M are in the convex hull of the columns of $M(:, \mathcal{K})$; in other words, the columns of $M(:, \mathcal{K})$ are the vertices of the convex hull of the columns of M . We can identify a vertex of this convex hull using the ℓ_2 norm as it must be maximized at a vertex. This is the main idea behind SPA which sequentially identifies the columns in \mathcal{K} as follows: at each step, it first extracts the column of M that has the largest ℓ_2 norm and then project all columns of M onto the orthogonal complement of the extracted column. Under the assumption that $M(:, \mathcal{K})$ is full column rank, SPA recovers the set \mathcal{K} .

Algorithm 3 generalizes SPA in a straightforward manner; we refer to it as generalized SPA (GSPA). At each iteration, it identifies a column or a row of M that will be used as a basis in a GS decomposition. Each iteration is made of two steps: First, it computes the norms of the columns of M multiplied by n and the norms of the rows of M multiplied by m , and select the row/column corresponding to the largest value. Second, it projects the columns/rows of M onto the orthogonal complement of the selected column/row.

One can check that the computational cost of GSPA is $\mathcal{O}(mnr)$ operations; the main operations being matrix-vector products. As for SPA, GSPA should be applied to a scaled GS matrix. Unfortunately, as opposed to SPA, there is no guarantee that a column (resp. row) with maximum ℓ_2 norm will belong to the set \mathcal{K}_1 (resp. \mathcal{K}_2); see Example 1 below. Hence GSPA is a heuristic for GS-NMF. However, we believe it could be possible to show that GSPA works under suitable additional conditions; this is a topic for further research. In fact, as we will see for the synthetic data experiments, GSPA works remarkably well for some randomly generated GS matrices.

Example 1. *Let us consider the following (2,2)-separable matrix*

$$M = \begin{pmatrix} W_1 & W_1 H_1 + W_2 H_2 \\ 0 & H_2 \end{pmatrix}, \text{ with } W_1 = \begin{pmatrix} 1 & \epsilon \\ 1 & 2 \\ 1 & 3 \end{pmatrix}, H_1 = \begin{pmatrix} \epsilon & 2\epsilon & 3\epsilon \\ \epsilon & 1 & 2 \end{pmatrix},$$

Algorithm 3 Generalized Successive Projection Algorithm (GSPA)

Input: A scaled matrix $M \in \mathbb{R}_+^{m \times n}$, number r of features to extract.

Output: A set $\mathcal{K}_1 \subset \{1, 2, \dots, n\}$ of column indices and $\mathcal{K}_2 \subset \{1, 2, \dots, m\}$ of row indices.

```

1: Let  $R = M$ ,  $\mathcal{K}_1 = \{\}$ ,  $\mathcal{K}_2 = \{\}$ .
2: while  $R \neq 0$  and  $|\mathcal{K}_1| + |\mathcal{K}_2| \leq r$  do
3:    $p = \operatorname{argmax}_{1 \leq j \leq n} n \|R(:, j)\|_2^2$ ;
4:    $q = \operatorname{argmax}_{1 \leq i \leq m} m \|R(i, :)\|_2^2$ ;
5:   if  $n \|R(:, p)\|_2^2 \geq m \|R(q, :)\|_2^2$  then
6:      $R = \left( I - \frac{R(:, p) R^T(:, p)}{\|R(:, p)\|_2^2} \right) R$ ;
7:      $\mathcal{K}_1 = \mathcal{K}_1 \cup \{p\}$ ;
8:   else
9:      $R^T = \left( I - \frac{R(q, :)^T R(q, :)}{\|R(q, :)\|_2^2} \right) R^T$ ;
10:     $\mathcal{K}_2 = \mathcal{K}_2 \cup \{q\}$ ;
11:   end if
12: end while
```

$H_2 = W_1^T$, $W_2 = H_1^T$. For $\epsilon = 0.001$, we have

$$M = \begin{pmatrix} 1 & 0.001 & 0.002 & 0.006 & 0.009 \\ 1 & 2 & 0.006 & 4.004 & 7.005 \\ 1 & 3 & 0.009 & 7.005 & 12.006 \\ 0 & 0 & 1 & 1 & 1 \\ 0 & 0 & 0.001 & 2 & 3 \end{pmatrix}.$$

Using SPA, one can check that M is not $(4,0)$ - nor $(0,4)$ -separable. Since there is no pattern of zeros of dimension $(1,3)$ or $(3,1)$, it is not $(1,3)$ - nor $(3,1)$ -separable (see Property 1). Therefore, $\mathcal{K}_1 = \{1, 2\}$ and $\mathcal{K}_2 = \{5, 6\}$ is the only possible GS decomposition with $|\mathcal{K}_1| + |\mathcal{K}_2| = 4$. The scaled version of M is

$$M_s = \begin{pmatrix} 4.654 & 0.028 & 0.251 & 0.034 & 0.033 \\ 0.212 & 2.551 & 0.034 & 1.045 & 1.157 \\ 0.134 & 2.421 & 0.033 & 1.157 & 1.255 \\ 0 & 0 & 4.654 & 0.212 & 0.134 \\ 0 & 0 & 0.028 & 2.551 & 2.421 \end{pmatrix}.$$

The column with largest ℓ_2 norm is the third which is not in \mathcal{K}_1 , and the row with the largest ℓ_2 norm is the first which is not in \mathcal{K}_2 ; they both have the same norm. Therefore, GSPA fails: it returns $\mathcal{K}_1 = \{1, 2, 3\}$ and $\mathcal{K}_2 = \{5\}$, or $\mathcal{K}_1 = \{2\}$ and $\mathcal{K}_2 = \{1, 4, 5\}$ (rows and columns of M_s are the same up to permutations, because $H_2 = W_1^T$ and $H_1 = W_2^T$).

Note however that the matrix is almost $(3,1)$ - and $(1,3)$ -separable. In fact,

$$\frac{\min_{P_1, P_2 \geq 0} \|M - M(:, 1:3)P_1 - P_2M(5, :)\|_F}{\|M\|_F} = 0.0244\%.$$

Note also that the model (11) applied on M_s identifies X and Y perfectly, with the form of (4).

5 Numerical Experiments

In this section, we conduct experiments on synthetic (Section 5.1), document (Section 5.2) and image data sets (Section 5.3) to test the performance of the proposed models. All experiments were run on Intel(R) Core(TM) i5-5200 CPU @2.20GHZ with 8GB of RAM using Matlab.

Since GS-NMF has not been considered before, we cannot compare GS-FGM and GSPA to existing GS-NMF algorithms. Instead, we consider the following state-of-the-art separable NMF algorithms:

- The successive projection algorithm (SPA); see the description in Section 4.
- The successive nonnegative projection algorithm (SNPA) [13] which works exactly as SPA except that it performs the projection taking the nonnegativity constraint into account.
- XRAY [22] which works similarly as SNPA except that it uses the unnormalized matrix M hence identifies the extreme rays of the cone generated by the columns of M . SPA and SNPA work on the scaled input matrix (columns are normalized to have unit ℓ_1 norm).
- FGNSR [18] which is the restriction of GS-FGM setting $Y = 0$.

Separable NMF algorithms can only identify a subset of the columns of the input matrix M . Hence, for each algorithm, we consider the following three possibilities:

1. The separable NMF algorithm is applied on M to identify r_1 important columns of M , and then on M^T to identify r_2 important rows of M . We refer to this variant as the name of the original algorithm + *; for example SPA*.
2. The separable NMF algorithm is applied on M to identify $r = r_1 + r_2$ columns of M . We refer to this variant using the name of the algorithm + C; for example SPA-C.
3. The separable NMF algorithm is applied on M^T to identify $r = r_1 + r_2$ rows of M . We refer to this variant as the name of the algorithm + R; for example SPA-R.

Although the last two possibilities will not be able to tackle GS-NMF, it is interesting to include them in the comparison to see how much GS-NMF algorithms can reduce the approximation error compared to separable NMF algorithms.

We have used a stopping criterion for GS-FGM based on the evolution of the iterates and the error: we stop GS-FGM when one of the following conditions holds:

$$\frac{e(k) - e(k-1)}{e(k-1)} \leq \delta \quad \text{or} \quad \|Z^{(k+1)} - Z^{(k)}\|_F \leq \delta \|Z^{(1)} - Z^{(0)}\|_F,$$

where $e(k)$ is the objective function at iteration k , $Z^{(k)} = (X^{(k)}, Y^{(k)})$ is the solution at iteration k , and $0 < \delta < 1$ is a parameter. We will use $\delta = 10^{-4}$ for synthetic data sets and $\delta = 10^{-2}$ for the real data sets (documents and images).

The code is available from <https://sites.google.com/site/nicolasgillis/code>.

5.1 Synthetic data sets

In this section, we compare the different algorithms on two types of synthetic data sets: fully randomly generated (Section 5.1.1), and the so-called middle-point experiment with adversarial noise (Section 5.1.2).

For GS-FGM, we identify the subsets \mathcal{K}_1 and \mathcal{K}_2 by using the r_1 largest diagonal entries of X and r_2 largest diagonal entries of Y , respectively. In all experiments, we run GS-FGM with the parameter $\lambda = 0.25$ and $\text{maxiter} = 1000$.

Given the subsets $(\mathcal{K}_2, \mathcal{K}_2)$ computed by an algorithm, we will report the following two quality measures:

1. The accuracy, defined as

$$\text{accuracy} = \frac{|\mathcal{K}_1^* \cap \mathcal{K}_1| + |\mathcal{K}_2^* \cap \mathcal{K}_2|}{|\mathcal{K}_1^*| + |\mathcal{K}_2^*|},$$

where \mathcal{K}_1^* and \mathcal{K}_2^* are the true column and row indices used to generate M . The accuracy reports the proportion of correctly identified row and column indices.

2. The relative approximation quality, defined as one minus the relative approximation error:

$$1 - \frac{\min_{P_1 \geq 0, P_2 \geq 0} \|M - M(:, \mathcal{K}_1)P_1 - P_2M(\mathcal{K}_2, :)\|_F}{\|M\|_F}. \quad (14)$$

Note that we compute P_1 and P_2 using the coordinate descent method from [15].

These two measures are between 0 and 1, 1 being the best possible value and 0 the worst.

5.1.1 Fully randomly generated data

We generate noisy (5,5)-separable matrices $M \in \mathbb{R}^{200 \times 150}$ as follows:

$$\Pi_r^T M \Pi_c^T = \max \left(0, D_r \left(\underbrace{\begin{pmatrix} W_1 & W_1 H_1 + W_2 H_2 \\ 0_{5,5} & H_2 \end{pmatrix}}_{M^s} \right) D_c + N \right),$$

where

- The entries of the matrices $W_1 \in \mathbb{R}^{195 \times 5}$, $H_1 \in \mathbb{R}^{195 \times 5}$, $W_2 \in \mathbb{R}^{195 \times 5}$, and $H_2 \in \mathbb{R}^{195 \times 5}$ are generated uniformly at random in the interval $[0,1]$ using the `rand` function of MATLAB.
- The diagonal matrices D_r and D_c are computed so that M^s is scaled; we use the algorithm that alternatively scales the columns and rows of the input matrix [21, 30].
- The entries of the noise $N \in \mathbb{R}^{200 \times 150}$ are generated uniformly at random with the normal distribution of mean 0 and standard deviation 1 using the `randn` function of MATLAB. The noise matrix N is then normalized so that

$$\|N\|_F = \epsilon \|M^s\|_F,$$

where M^s is the noiseless scaled (5,5)-separable matrix, and ϵ is a parameter that relates to the noise level.

- Π_r and Π_c are random permutation matrices.

For each noise level $\epsilon = \frac{2}{25}i$ for $0 \leq i \leq 25$ so that $\epsilon \in [0, 2]$, we generate 25 such matrices and report the average quality measures on Figures 1 and 2.

We observe the following:

- As expected, the variants of separable NMF algorithms extracting only columns or rows have an accuracy of at most 50%. However, even in terms of approximation quality, they perform worse, with 4% to 8% higher relative error for low noise levels ($\epsilon \leq 0.3$). This validates the GS-NMF model in the sense that it is able to reduce the reconstruction error compared to separable NMF for the same factorization rank.

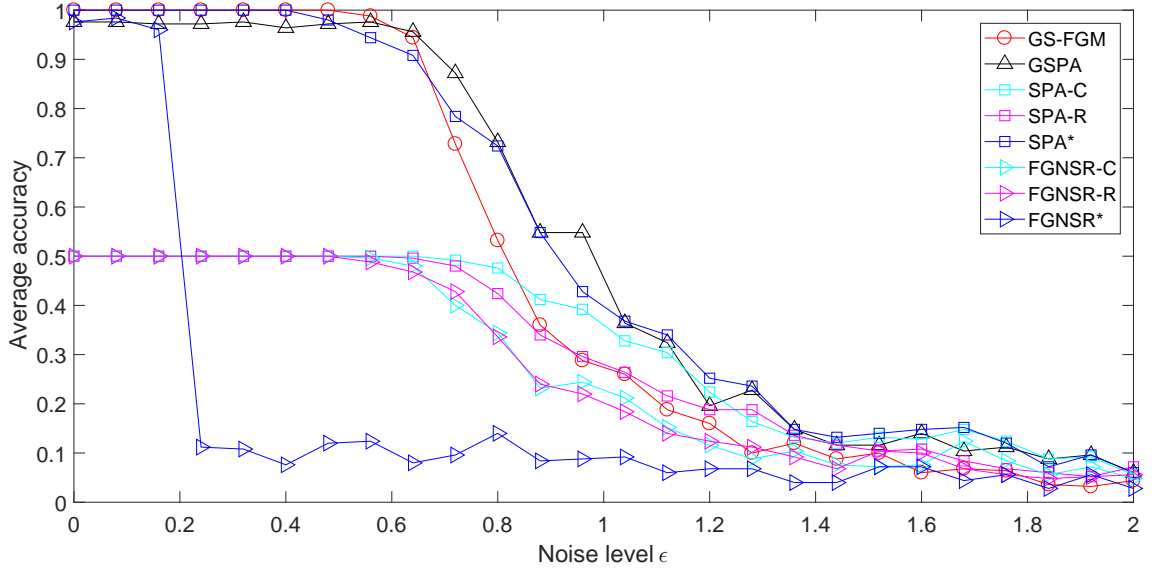


Figure 1: Average accuracy for the different algorithms on the fully randomly generated GS matrices. It has to be noted that SNPA and XRAY variants perform exactly the same as SPA variants, hence we do not display them on this figure for clarity.

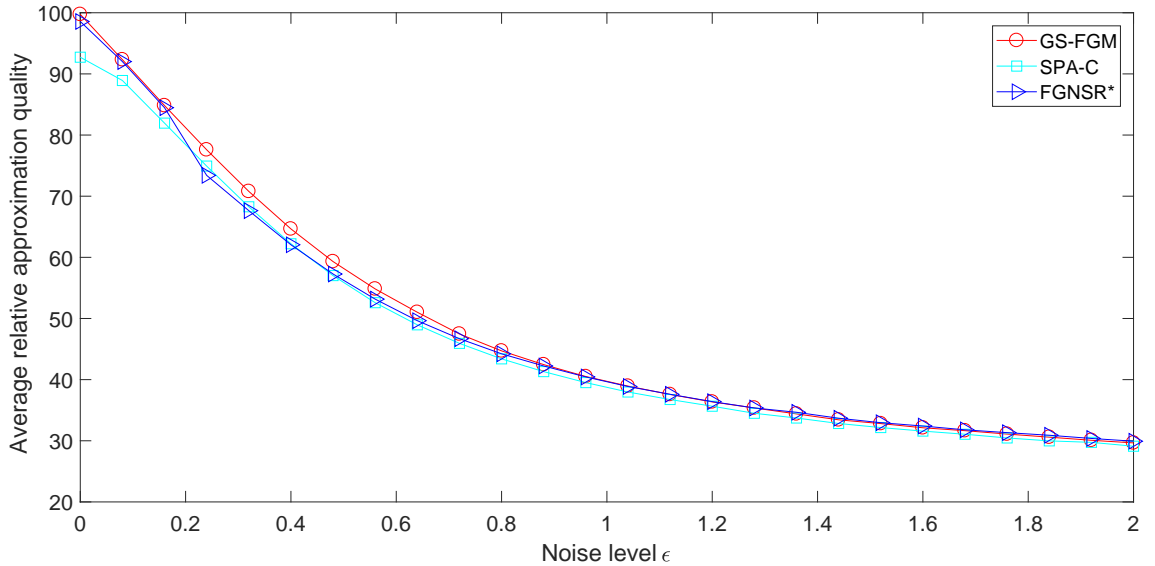


Figure 2: Average relative approximation quality in % on the fully randomly generated GS matrices. We only display the curves for three algorithms because it is difficult to visualize all curves simultaneously. It has to be noted that: (i) the curves of GSPA, SPA*, SNPA* and XRAY* are almost the same as for GS-NMF, and (ii) the curves of SPA-R, SNPA-C, SNPA-R, XRAY-C, XRAY-R, FGNSR-C and FGNSR-R are almost the same as for SPA-C.

- In terms of accuracy, GS-FGM performs the best, having an accuracy of 100% for all $\epsilon \leq 0.48$. Surprisingly, even for low noise levels, GSPA is not able to recover exactly the column and row indices although the approximation quality is very close to that of GS-FGM. Separable NMF algorithms used to recover r_1 columns and r_2 rows perform well, almost as well as GS-FGM (except for FGNSR* whose performance drops rapidly).

Since the performance of GS-FGM is only slightly better than SPA*, one may wonder whether GS-FGM is really useful. Shouldn't we simply use SPA* that is computationally much cheaper? In the next section, we construct more complicated synthetic data sets for which GS-FGM and GSPA outperforms the separable NMF algorithms showing that, in fact, GS-FGM and GSPA are useful to tackle GS-NMF.

5.1.2 Middle points and adversarial noise

In this section, we generate the noisy GS matrices exactly as in the previous section except that $m = 78$, $n = 55$, $r_1 = 10$, $r_2 = 12$, and

- the $\binom{r_1}{2} = 45$ columns H_1 (resp. $\binom{r_2}{2} = 66$ rows of W_2) contain all possible combinations of two non-zero entries equal to 0.5 at different positions. Hence, the columns of $W_1 H_1$ (resp. rows of $W_2 H_2$) are all the middle points of the columns of W_1 (resp. rows of H_2).
- No noise is added to the first r_1 columns and last r_2 rows of M^s , that is, $N(:, 1 : r_1) = 0$ and $N(m - r_2 + 1 : m, :) = 0$, while we set

$$N(1 : m - r_2, r_1 + 1 : n) = M^s(1 : m - r_2, r_1 + 1 : n) - \bar{w}e^T - e\bar{h},$$

where \bar{w} and \bar{h} are the average of the columns of W_1 and rows of H_2 , respectively, that is, $\bar{w} = \frac{1}{r_1} W_1 e$ and $\bar{h} = \frac{1}{r_2} e^T H_2$. Intuitively, the noise will move the data point towards the outside of the convex hull of the columns of W_1 and the rows of H_2 . The noise matrix N is normalized so that

$$\|N\|_F = \epsilon \|M^s\|_F.$$

This example is inspired by the so-called middle point experiment from [19]. Intuitively, we are moving the data points towards the outside the points that can be spanned by W_1 and H_2 .

For each noise level $\epsilon = \frac{i}{25}$ for $0 \leq i \leq 25$, we generate 25 such matrices and we generate 25 such matrices and report the average quality measures on Figures 3 and 4.

We observe the following:

- No separable NMF algorithm is able to identify the column and row indices properly, even in the absence of noise.
- GSPA and GS-FGM are both able to recover the row and column indices, while GS-FGM is able to do so for higher noise levels hence is more robust to noise for these data sets.
- For low noise levels ($\epsilon \leq 0.2$) GSPA and GS-FGM produce solutions with much lower reconstruction error than the separable NMF algorithms (more than 10% lower). Moreover, for slightly higher noise levels ($0.2 \leq \epsilon \leq 0.3$), GS-FGM performs best, with about 5% lower relative error than GSPA, and 10% compared to separable NMF algorithms.

This second synthetic data experiments shows the superiority of GS-NMF compared to separable NMF: GS-NMF allows to identify low-rank factorization with much lower reconstruction error. Although this was expected, this validates the usefulness of GS-NMF. Among GS-NMF algorithms, GS-FGM performs best producing solutions with lower reconstruction error than GSPA.

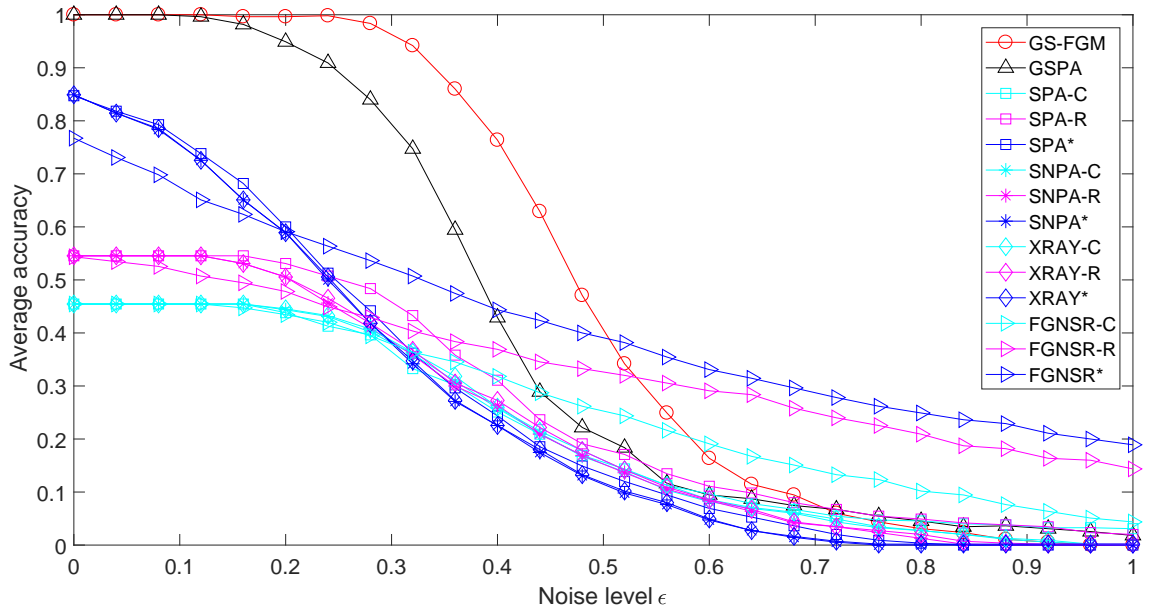


Figure 3: Average accuracy for the different algorithms on the middle-point GS matrices with adversarial noise.

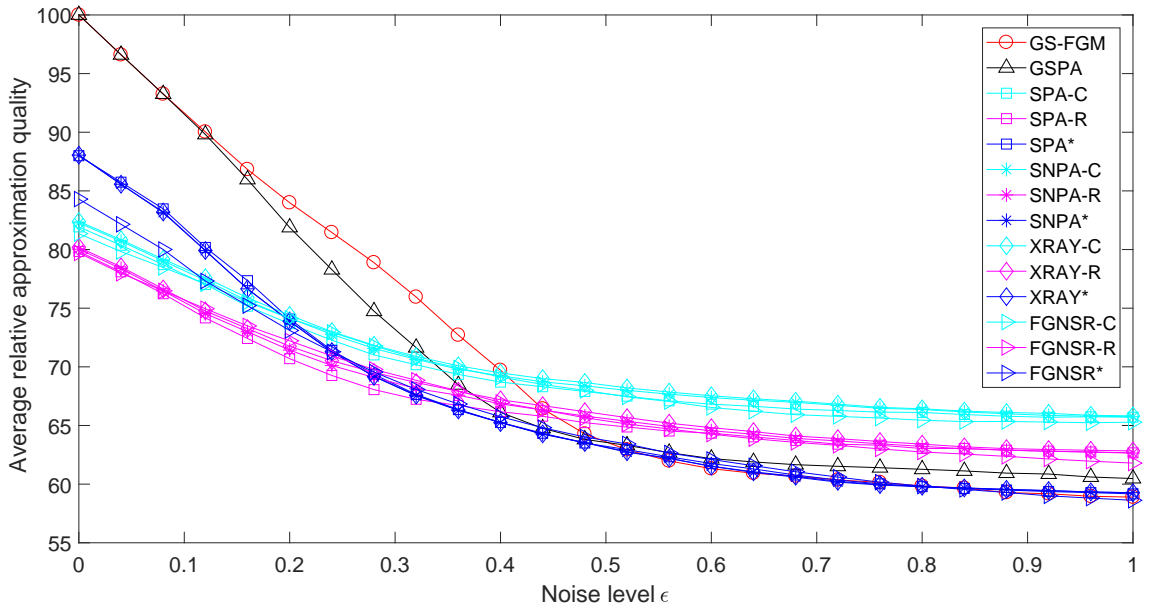


Figure 4: Average relative approximation quality in % for the different algorithms on the middle-point GS matrices with adversarial noise.

5.2 Document data sets

In this section, we compare the different algorithms on documents data sets. We use the TDT30 data set [6], and the 14 data sets from [37]. Note that document data sets are sparse hence are not necessarily scalable hence we did not scale the input matrix.

For GS-FGM, we try 10 different values of λ chosen in $[10^{-3}, 10]$ with 10 log-spaced values (in Matlab, `logspace(-3,1,10)`), and keep the solution with the highest approximation quality. As opposed to the synthetic data sets, the numbers r_1 and r_2 are unknown. To evaluate (r_1, r_2) when using GS-FGM, we use the strategy described in Section 3.2 for real data sets.

Subsampling For the document data sets, the size of input data matrix can be very large (the number of words is typically of the order of 10^4). It is impractical to apply GS-FGM such data sets since GS-FGM runs in $\mathcal{O}(mn^2 + nm^2)$ operations. Similarly as done in [18], we preselect a subset of columns and rows of the input matrix. To do so, we adopt the hierarchical clustering from [16], running on average in $\mathcal{O}(mn \log_2 C)$, where C is the number of the clusters to generate. For tr11 and tr23 data sets, since the number of documents is relatively small (414 for tr11, 204 for tr23), we keep all the documents and extract 500 words. For Newsgroups 20, which is a very large data set, we only consider the first 10 classes and refer to the corresponding data set as NG10. For the other data sets, we extract 500 documents and 500 words, and consider a submatrix matrix $M_s \in \mathbb{R}^{500 \times 500}$. However, we take into account the importance of each selected column and row by identifying the the number of data points attached to it (this is given by the hierarchical clustering). To do so, we scale it using the square root of the number of points belonging to its cluster.

Finally, each algorithm will identify a subset of r_1 columns and r_2 rows of the subsampled matrix. From these subsets, we identify the corresponding columns and rows of the original matrix, and Table 1 reports the approximation quality (14) of the different algorithms. It also reports the approximation quality of the rank- r truncated SVD, that is, $1 - \frac{\|M - M_r\|_F}{\|M\|_F}$ where M_r is the best rank- r approximation of M , to serve as a reference. To limit the number of algorithms, we only use SPA-R and SPA-C variants when it comes to extracting only rows and columns, respectively. We also only run the separable NMF variants extracting r_1 columns and r_2 rows using the values of (r_1, r_2) identified by GS-FGM.

Dataset	r	(r_2, r_1)	GSPA	(r_2, r_1)	GS-FGM	SPA*	SNPA*	XRAY*	FGNSR*	SPA-C	SPA-R	SVD
NG10	10	(7,3)	<u>91.61</u>	(8,2)	91.64	91.35	91.35	90.97	91.25	91.44	91.49	92.46
TDT30	30	(7,23)	14.13	(4,26)	<u>14.38</u>	14.03	14.03	10.37	13.17	14.47	11.30	18.48
classic	4	(4,0)	3.58	(4,0)	3.58	3.58	3.58	1.29	2.07	3.58	1.48	5.20
reviews	5	(0,5)	8.39	(0,5)	8.39	8.39	8.39	5.79	8.24	8.39	7.69	13.48
sports	7	(0,7)	10.49	(1,6)	10.65	10.65	10.65	4.32	9.90	10.49	5.98	13.76
ohscal	10	(0,10)	10.27	(0,10)	10.27	10.27	10.27	4.57	9.96	10.27	7.03	11.49
k1b	6	(1,5)	5.76	(1,5)	7.07	5.62	5.62	2.42	5.67	<u>5.78</u>	4.54	9.62
la12	6	(0,6)	<u>4.79</u>	(0,6)	<u>4.79</u>	<u>4.79</u>	<u>4.79</u>	1.45	4.88	<u>4.79</u>	3.02	7.78
hitech	6	(3,3)	6.43	(3,3)	6.43	4.50	4.50	2.52	3.36	5.77	4.86	8.99
la1	6	(1,5)	5.05	(2,4)	5.13	4.51	4.51	2.43	4.55	<u>5.11</u>	3.73	8.03
la2	6	(0,6)	5.86	(0,6)	5.86	5.86	5.86	2.55	5.77	5.86	3.90	8.35
tr41	10	(5,5)	52.30	(7,3)	<u>54.90</u>	53.31	53.31	51.12	53.12	53.12	56.03	57.74
tr45	10	(5,5)	69.08	(7,3)	71.94	68.20	68.20	61.83	65.90	68.37	69.55	76.36
tr11	9	(6,3)	74.21	(7,2)	<u>74.27</u>	72.14	72.14	57.15	70.84	72.50	74.74	76.44
tr23	6	(1,5)	63.660	(5,1)	<u>70.70</u>	68.46	68.46	68.46	68.46	65.04	71.32	72.86

Table 1: The relative approximation quality for the document data sets. The highest quality is highlighted in bold, the second highest is underlined.

We observe the following:

- GS-FGM and GSPA provide the same solutions in 6 out of the 15 cases. In 5 out of these 6 cases, SPA* and SNPA* also provide the same solutions.
- As opposed to the synthetic data sets, SPA-C and SPA-R sometimes perform best, although never significantly better than GS-FGM.
- GS-FGM performs on average the best, having in all cases the highest or second highest relative approximation quality.

Table 2 reports the computational time for the different algorithms. As expected, GS-FGM and FGNSR are slower but the computational time is reasonable for such matrices (below 2.5 seconds).

Dataset	r	(r_2, r_1)	GSPA	(r_2, r_1)	GS-FGM	SPA*	SNPA*	XRAY*	FGNSR*	SPA-C	SPA-R	SVD
NG10	10	(7,3)	0.117	(8,2)	0.586	0.015	0.321	0.201	1.052	0.009	0.014	0.055
TDT30	30	(7,23)	0.333	(4,26)	2.541	0.022	0.882	0.503	0.720	0.027	0.021	0.070
classic	4	(4,0)	0.038	(4,0)	0.932	0.009	0.105	0.051	0.191	0.005	0.008	0.028
reviews	5	(0,5)	0.048	(0,5)	2.080	0.009	0.078	0.059	0.275	0.005	0.009	0.031
sports	7	(0,7)	0.058	(1,6)	1.301	0.023	0.108	0.100	0.398	0.008	0.009	0.033
ohscal	10	(0,10)	0.078	(0,10)	1.761	0.008	0.150	0.109	0.274	0.008	0.010	0.046
k1b	6	(1,5)	0.053	(1,5)	0.984	0.013	0.076	0.080	0.312	0.006	0.007	0.031
la12	6	(0,6)	0.052	(0,6)	1.274	0.007	0.089	0.078	0.178	0.007	0.007	0.025
hitech	6	(3,3)	0.052	(3,3)	2.291	0.013	0.118	0.103	0.272	0.006	0.012	0.018
la1	6	(1,5)	0.142	(2,4)	0.928	0.012	0.077	0.080	0.348	0.005	0.010	0.024
la2	6	(0,6)	0.051	(0,6)	1.377	0.008	0.110	0.067	0.266	0.007	0.008	0.026
tr41	10	(5,5)	0.099	(7,3)	0.473	0.023	0.115	0.107	1.000	0.007	0.015	0.016
tr45	10	(5,5)	0.137	(7,3)	1.636	0.012	0.166	0.115	0.663	0.006	0.018	0.020
tr11	9	(6,3)	0.094	(7,2)	0.345	0.013	0.083	0.078	0.676	0.004	0.010	0.013
tr23	6	(1,5)	0.008	(5,1)	0.220	0.006	0.032	0.028	0.262	0.004	0.003	0.009

Table 2: Computational time in seconds for the different algorithms on the document datasets.

5.3 Facial image data sets

In this section, the algorithms are applied on facial image data sets. In this context, GS-NMF will identify important subjects and important pixels that allow to reconstruct as best as possible the original images. We use the following facial image data sets:

- The CBCL data set is a public database for research usage provided by the MIT center for Biological and Computation Learning. It consists 2429 face images of size 19×19 so that the input pixel-by-face matrix has dimension 361×2429 . We set $r = 49$ as in [23].
- The Frey data set is collected by Brendan Frey. It contains 1965 images of Brendan’s face and the size of each image is 20×28 so that the input pixel-by-face matrix has dimension 560×1965 . We set $r = 50$.
- The Yale data set contains 38 individuals, each of which as 64 frontal face images under different lighting conditions. The images are size of 192×168 which is too large for our purpose (see the discussion in the previous section) hence all the images are downsampled to have size 48×42 . We also select 10 face images from each individual randomly and obtain 380 images. Finally, the pixel-by-face matrix has dimension 2016×380 . We set $r = n/10 = 38$.
- The ORL data set contains a set of faces taken between April 1992 and April 1994 at the Olivetti Research Laboratory in Cambridge, UK. There are ten different images of each of the 40 distinct subjects, each image is size of 112×92 . We subsample each image to obtain images of size 23×19 . The pixel-by-face matrix has dimension 437×400 . We set $r = n/10 = 40$.

Note that the factorization ranks were chosen rather arbitrarily; we refer the reader to [33] for a discussion on the choice of r . We use the same strategy to tune λ as for document data sets. To give each facial image the same importance, we scale them so that their ℓ_1 norm is equal to one. The relative approximation quality of the factorizations provided by the different algorithms are reported in Table 3.

Dataset	r	(r_2, r_1)	GSPA	(r_2, r_1)	GS-FGM	SPA*	SNPA*	XRAY*	FGNSR*	SPA-C	SPA-R	SVD
CBCL	49	(1,48)	80.73	(14,35)	<u>83.10</u>	82.29	82.11	82.33	74.40	79.44	84.57	91.40
Frey	50	(24,26)	82.46	(39,11)	<u>83.89</u>	83.43	<u>83.89</u>	84.15	78.87	80.61	83.78	91.51
Yale	38	(13,25)	57.52	(24,14)	68.26	61.10	59.70	60.91	44.42	60.24	<u>62.94</u>	79.23
ORL	40	(20,20)	81.38	(28,12)	82.54	82.32	82.49	<u>82.58</u>	78.75	82.23	83.26	90.24

Table 3: The relative approximation quality for the facial image data sets. The highest quality is highlighted in bold, the second highest is underlined.

For these data sets, GS-FGM outperforms GSPA. However, SPA-R works very well, slightly better than GS-FGM on CBCL and ORL databases and worse on the Frey and Yale data sets. The reason is that extracting representative faces within a set of images is not always very appropriate because of the nonnegativity constraints. In some sense, the GS-NMF model is not ideal in this situation, but it is still able to provide meaningful results; for example, for the Yale data sets, it provides significantly lower approximation error than all other algorithms. Here the non-uniqueness issue plays a role. For example, on the Frey data set, we see that using a (0,49)-separable approximation (SPA-R) leads to an error very close to a (35,14)-separable approximation (GS-FGM).

Figures 5, 7, 9 and 11 provide a visual representations of the solutions generated by GS-FGM: for each data set, they display the positions of the selected pixels and the selected representative faces. It is interesting to observe the location of the selected pixels: they are either located on the edge (where pixels behave rather differently, not being part of the faces) or are well spread around the center of the face. The selected faces represent rather different faces from the data sets. For the CBCL and ORL data sets, the selected faces either come from different persons that look rather different, or of the same person in very different positions or with different illuminations (Figures 5 and 11). For the Frey data sets, the selected faces represent different emotions (Figure 7). For the Yale data sets, the selected faces represent different persons and illuminations (Figure 9).

Figures 6, 8, 10, and 12 display some sample images from the different data sets and their reconstruction using GS-FGM.



Figure 5: The first image highlights the 14 extracted pixels by GS-FGM for the CBCL data set. The next images are the 35 subjects extracted by GS-FGM.



Figure 6: The first row displays some images of the CBCL data set, the second row displays their approximation by the separable part $M(:, \mathcal{K}_1)P_1$ using the extracted faces, the third row displays their approximation by the separable part $P_2M(\mathcal{K}_2, :)$ using the extracted pixels, the last row is the GS approximation $M(:, \mathcal{K}_1)P_1 + P_2M(\mathcal{K}_2, :)$.



Figure 7: The first image highlights the 39 extracted pixels by GS-FGM for the Frey data set. The next images are the 11 subjects extracted by GS-FGM.



Figure 8: The first row displays some images of the Frey data set, the second row displays their approximation by the separable part $M(:, \mathcal{K}_1)P_1$ using the extracted faces, the third row displays their approximation by the separable part $P_2M(\mathcal{K}_2, :)$ using the extracted pixels, the last row is the GS approximation $M(:, \mathcal{K}_1)P_1 + P_2M(\mathcal{K}_2, :)$.

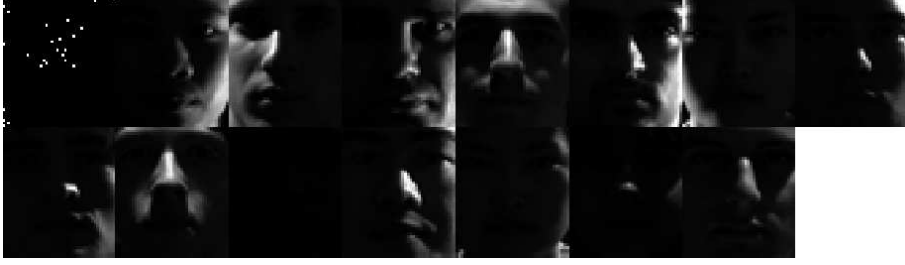


Figure 9: The first image highlights the 24 extracted pixels by GS-FGM for the Yale data set. The next images are the 14 subjects extracted by GS-FGM.



Figure 10: The first row displays some images of the Yale data set, the second row displays their approximation by the separable part $M(:, \mathcal{K}_1)P_1$ using the extracted faces, the third row displays their approximation by the separable part $P_2M(\mathcal{K}_2, :)$ using the extracted pixels, the last row is the GS approximation $M(:, \mathcal{K}_1)P_1 + P_2M(\mathcal{K}_2, :)$.



Figure 11: The first image highlights the 28 extracted pixels by GS-FGM for the ORL data set. The next images are the 12 subjects extracted by GS-FGM.

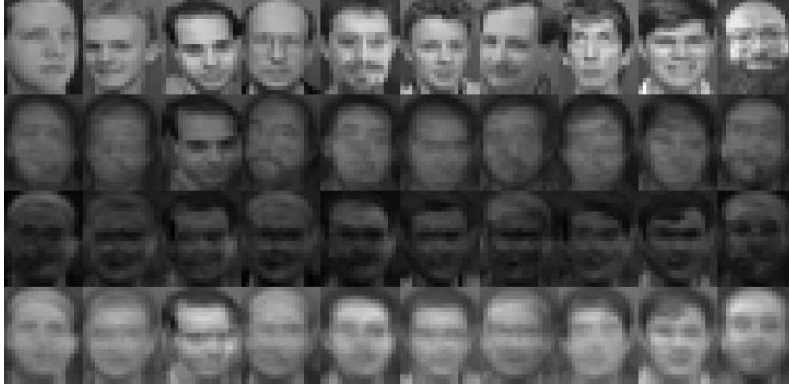


Figure 12: The first row displays some images of the ORL data set, the second row displays their approximation by the separable part $M(:, \mathcal{K}_1)P_1$ using the extracted faces, the third row displays their approximation by the separable part $P_2M(\mathcal{K}_2, :)$ using the extracted pixels, the last row is the GS approximation $M(:, \mathcal{K}_1)P_1 + P_2M(\mathcal{K}_2, :)$.

Table 4 reports the computational time for the different algorithms. As expected, GS-FGM and FGNSR are slower; in particular for the largest data set, namely the Yale data set (2016×380), where GS-FGM requires 35 seconds.

Dataset	r	(r_2, r_1)	GSPA	(r_2, r_1)	GS-FGM	SPA*	SNPA*	XRAY*	FGNSR*	SPA-C	SPA-R	SVD
CBCL	49	(1,48)	1.612	(14,35)	5.076	0.075	4.387	22.092	25.559	0.070	0.128	0.605
Frey	50	(24,26)	2.616	(39,11)	5.387	0.096	2.995	10.450	5.151	0.070	0.090	0.603
Yale	38	(13,25)	1.387	(24,14)	35.746	0.053	1.672	2.165	7.003	0.048	0.044	0.318
ORL	40	(20,20)	0.470	(28,12)	0.905	0.017	1.173	4.056	1.187	0.013	0.013	0.051

Table 4: Computational time in seconds for the different algorithms on the image data sets.

6 Conclusion

In this paper, we have generalized separable NMF: instead of only selecting columns of the input matrix to approximate it, we allow for columns and rows to be selected. We refer to this problem as generalized separable NMF (GS-NMF). We studied some interesting properties of matrices that can be decomposed using GS-NMF; they are referred to as GS matrices. In particular, we showed that, as opposed to separable NMF, GS decompositions are not necessarily unique. We also showed that GS-NMF can represent matrices much more compactly than separable NMF. Then, we proposed a convex optimization model to tackle GS-NMF, and developed a fast gradient method to solve the model. We also proposed a heuristic algorithm inspired by the successive projection algorithm from the separable NMF literature. We compared the algorithms on synthetic, document and image data sets and showed that they are able, in most cases, to generate decompositions with smaller reconstruction error than separable NMF algorithms.

Further work include to deepen our understanding of GS matrices. This would hopefully allow for example to design more efficient algorithms that provably recover optimal decompositions under suitable conditions (e.g., uniqueness) and in the presence of noise; as done for separable NMF algorithms.

References

- [1] M. C. U. Araújo, T. C. B. Saldanha, R. K. H. Galvao, T. Yoneyama, H. C. Chame, and V. Visani. The successive projections algorithm for variable selection in spectroscopic multicomponent analysis. *Chemometrics and Intelligent Laboratory Systems*, 57(2):65–73, 2001.
- [2] S. Arora, R. Ge, Y. Halpern, D. Mimno, A. Moitra, D. Sontag, Y. Wu, and M. Zhu. A practical algorithm for topic modeling with provable guarantees. In *International Conference on Machine Learning*, pages 280–288, 2013.
- [3] S. Arora, R. Ge, R. Kannan, and A. Moitra. Computing a nonnegative matrix factorization—provably. In *Proceedings of the forty-fourth annual ACM symposium on Theory of computing*, pages 145–162. ACM, 2012.
- [4] S. Arora, R. Ge, R. Kannan, and A. Moitra. Computing a nonnegative matrix factorization—provably. *SIAM Journal on Computing*, 45(4):1582–1611, 2016.
- [5] S. Arora, R. Ge, and A. Moitra. Learning topic models—going beyond svd. In *Foundations of Computer Science (FOCS), 2012 IEEE 53rd Annual Symposium on*, pages 1–10. IEEE, 2012.
- [6] D. Cai, Q. Mei, J. Han, and C. Zhai. Modeling hidden topics on document manifold. In *Proceedings of the 17th ACM conference on Information and knowledge management*, pages 911–920. ACM, 2008.
- [7] O. Dikmen, Z. Yang, and E. Oja. Learning the information divergence. *IEEE Transactions on Pattern Analysis and Machine Intelligence*, 37(7):1442–1454, 2015.
- [8] E. Elhamifar, G. Sapiro, and R. Vidal. See all by looking at a few: Sparse modeling for finding representative objects. In *2012 IEEE Conference on Computer Vision and Pattern Recognition*, pages 1600–1607. IEEE, 2012.
- [9] E. Esser, M. Moller, S. Osher, G. Sapiro, and J. Xin. A convex model for nonnegative matrix factorization and dimensionality reduction on physical space. *IEEE Transactions on Image Processing*, 21(7):3239–3252, 2012.
- [10] C. Févotte, N. Bertin, and J.-L. Durrieu. Nonnegative matrix factorization with the itakura-saito divergence: With application to music analysis. *Neural computation*, 21(3):793–830, 2009.
- [11] X. Fu, K. Huang, N. D. Sidiropoulos, and W.-K. Ma. Nonnegative matrix factorization for signal and data analytics: Identifiability, algorithms, and applications. *IEEE Signal Processing Magazine*, 36(2):59–80, 2019.
- [12] N. Gillis. Robustness analysis of hottopixx, a linear programming model for factoring nonnegative matrices. *SIAM Journal on Matrix Analysis and Applications*, 34(3):1189–1212, 2013.
- [13] N. Gillis. Successive nonnegative projection algorithm for robust nonnegative blind source separation. *SIAM Journal on Imaging Sciences*, 7(2):1420–1450, 2014.
- [14] N. Gillis. The why and how of nonnegative matrix factorization. *Regularization, Optimization, Kernels, and Support Vector Machines*, 12:257–291, 2014.
- [15] N. Gillis and F. Glineur. Accelerated multiplicative updates and hierarchical als algorithms for non-negative matrix factorization. *Neural computation*, 24(4):1085–1105, 2012.
- [16] N. Gillis, D. Kuang, and H. Park. Hierarchical clustering of hyperspectral images using rank-two nonnegative matrix factorization. *IEEE Transactions on Geoscience and Remote Sensing*, 53(4):2066–2078, 2015.
- [17] N. Gillis and R. Luce. Robust near-separable nonnegative matrix factorization using linear optimization. *The Journal of Machine Learning Research*, 15(1):1249–1280, 2014.
- [18] N. Gillis and R. Luce. A fast gradient method for nonnegative sparse regression with self dictionary. *IEEE Transactions on Image Processing*, 27(1):24–37, 2018.
- [19] N. Gillis and S. A. Vavasis. Fast and robust recursive algorithms for separable nonnegative matrix factorization. *IEEE Transactions on Pattern Analysis and Machine Intelligence*, 36(4):698–714, 2014.

- [20] S. A. Goreinov, N. L. Zamarashkin, and E. E. Tyrtyshnikov. Pseudo-skeleton approximations by matrices of maximal volume. *Mathematical Notes*, 62(4):515–519, 1997.
- [21] P. A. Knight. The sinkhorn–knopp algorithm: convergence and applications. *SIAM Journal on Matrix Analysis and Applications*, 30(1):261–275, 2008.
- [22] A. Kumar, V. Sindhwani, and P. Kambadur. Fast conical hull algorithms for near-separable non-negative matrix factorization. In *International Conference on Machine Learning*, pages 231–239, 2013.
- [23] D. D. Lee and H. S. Seung. Learning the parts of objects by non-negative matrix factorization. *Nature*, 401:788–791, 1999.
- [24] G. Liu and S. Yan. Latent low-rank representation for subspace segmentation and feature extraction. In *2011 International Conference on Computer Vision*, pages 1615–1622. IEEE, 2011.
- [25] W.-K. Ma, J. M. Bioucas-Dias, T.-H. Chan, N. Gillis, P. Gader, A. J. Plaza, A. Ambikapathi, and C.-Y. Chi. A signal processing perspective on hyperspectral unmixing: Insights from remote sensing. *IEEE Signal Processing Magazine*, 31(1):67–81, 2014.
- [26] M. W. Mahoney and P. Drineas. Cur matrix decompositions for improved data analysis. *Proceedings of the National Academy of Sciences*, 106(3):697–702, 2009.
- [27] A. Mikhalev and I. V. Oseledets. Rectangular maximum-volume submatrices and their applications. *Linear Algebra and its Applications*, 538:187–211, 2018.
- [28] Y. Nesterov. A method of solving a convex programming problem with convergence rate $o(1/k^2)$. In *Soviet Mathematics Doklady*, volume 27, pages 372–376, 1983.
- [29] Y. Nesterov. *Introductory lectures on convex optimization: A basic course*, volume 87. Springer Science & Business Media, 2004.
- [30] R. A. Olshen and B. Rajaratnam. Successive normalization of rectangular arrays. *Annals of statistics*, 38(3):1638, 2010.
- [31] B. Recht, M. Fazel, and P. A. Parrilo. Guaranteed minimum-rank solutions of linear matrix equations via nuclear norm minimization. *SIAM Review*, 52(3):471–501, 2010.
- [32] B. Recht, C. Re, J. Tropp, and V. Bittorf. Factoring nonnegative matrices with linear programs. In *Advances in Neural Information Processing Systems*, pages 1214–1222, 2012.
- [33] V. Y. Tan and C. Févotte. Automatic relevance determination in nonnegative matrix factorization with the β -divergence. *IEEE Transactions on Pattern Analysis and Machine Intelligence*, 35(7):1592–1605, 2012.
- [34] L. Thomas. Rank factorization of nonnegative matrices. *SIAM Review*, 16(3):393–394, 1974.
- [35] K.-C. Toh, M. Todd, and R. Tütüncü. SDPT3—a MATLAB software package for semidefinite programming, version 1.3. *Optimization Methods and Software*, 11(1-4):545–581, 1999.
- [36] S. A. Vavasis. On the complexity of nonnegative matrix factorization. *SIAM Journal on Optimization*, 20(3):1364–1377, 2010.
- [37] S. Zhong and J. Ghosh. Generative model-based document clustering: a comparative study. *Knowledge and Information Systems*, 8(3):374–384, 2005.